DELPHI Collaboration

DELPHI 2003-048 CONF 668
June 25, 2003

Search for a fourth generation b'-quark at LEP-II at $\sqrt{s} = 196 - 209$ GeV

Preliminary

S. Andringa[1], N. Castro[1], M. Espírito-Santo[1], P. Gonçalves[1], O. Oliveira[2], S.M. Oliveira[3], A. Onofre[1,4], M. Pimenta[1], R. Santos[3], B. Tomé[1] and F. Veloso[1]

[1]LIP-IST-FCUL, Av. Elias Garcia, 14, 1, 1100-149 Lisboa, Portugal
[2]Dep. Física, Universidade de Coimbra, P-3004-516 Coimbra, Portugal
[3]Centro de Física Teórica e Computacional, FCUL,
Av. Prof. Gama Pinto, 2, 1649-003 Lisboa, Portugal
[4]UCP, R. Dr. Mendes Pinheiro, 24, 3080 Figueira da Foz, Portugal

Abstract

A search for pair production of fourth generation b'-quarks was performed using data taken by the DELPHI detector at LEP-II. The analysed data were collected at centre-of-mass energies ranging from 196 to 209 GeV, corresponding to an integrated luminosity of about 420 pb^{-1}. No evidence for a signal was found. Upper limits on $BR_{b' \to bZ}$ and $BR_{b' \to cW}$ were obtained at 95% confidence level for $m_{b'}$ ranging from 96 to 103 GeV/c^2. These limits, together with the theoretical branching ratios predicted by a sequential four generations model, were used to constraint the values of $|\frac{V_{cb'}}{V_{tb'}V_{tb}}|$, where $V_{cb'}$, $V_{tb'}$ and V_{tb} are elements of the extended 4×4 CKM matrix.

Contributed Paper for EPS 2003 (Aachen) and LP 2003 (FNAL)

1 Introduction

The Standard Model (SM) is in excellent agreement with experimental data [1], although it leaves some open questions. Among other parameters, the number of fermion generations and their mass spectrum are not explained by the SM. The measurement of the Z decay widths [1] establishes that the number of light ($m < m_Z/2$) neutrino species is three with an error below 1%. Nevertheless, it is also true that when one extra heavy generation is assumed, the fit to the electroweak data is as good as the one assuming three generations [2].

Extra generations of fermions are predicted in several SM extensions [3]. The heavy fourth generation fermions are supposed to carry the same quantum numbers as any family in the known spectrum. The sequential model [4] considers that the 4×4 Cabbibo-Kobayashi-Maskawa (CKM) matrix is unitary, approximately symmetric and almost diagonal. As CP-violation is not considered, all the CKM elements are assumed to be real. In the quark sector, an up-type quark, t', and a down-type quark, b', are included:

$$\begin{array}{c} Q = 2/3 \\ Q = -1/3 \end{array} \qquad \begin{pmatrix} u \\ d \end{pmatrix} \begin{pmatrix} c \\ s \end{pmatrix} \begin{pmatrix} t \\ b \end{pmatrix} \begin{pmatrix} \boldsymbol{t'} \\ \boldsymbol{b'} \end{pmatrix}. \tag{1}$$

The b'-quark may decay via charged currents (CC) to UW, with $U = t', t, c, u$, or via flavour changing neutral currents (FCNC) to DX, with $X = Z, H, \gamma, g$ and $D = b, s, d$ (Fig. 1). In the SM, FCNC are absent at tree level, but can naturally appear at one-loop level, due to CKM mixing.

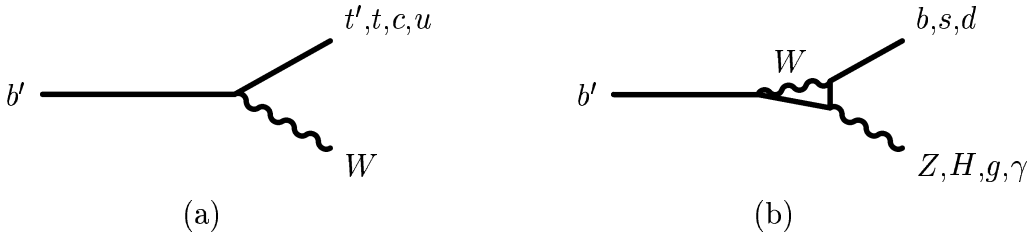

Figure 1: *Feynman diagrams corresponding to the (a) CC and (b) FCNC b' decay modes.*

The mass difference $|m_{t'} - m_{b'}|$ is expected to be below 60 GeV [3, 5]. If the b' is lighter than both the t' and the t, the CC decays $b' \to t'W$ and $b' \to tW$ are kinematically forbidden. In particular, when $m_Z < m_{b'} < m_H$ the $b' \to cW$ and $b' \to bZ$ decays are expected to be dominant [5, 6, 7]. In this case, the partial widths of the CC and FCNC b' decays depend mainly on $R_{CKM} = |\frac{V_{cb'}}{V_{tb'}V_{tb}}|$ and on the b' and t' masses [7].

At LEP-I, all the experiments searched for the pair production of b'-quarks ($e^+e^- \to b'\bar{b'}$), giving a lower mass limit on the b' mass close to half the Z mass [8]. At the TEVATRON both the DØ and the CDF experiments searched for b' pair production. Mass limits were obtained under assumptions for the branching ratios (BR) of the studied b' decays. DØ [9] found a lower limit of 128 GeV/c^2 assuming $BR_{b' \to cW} = 1$ and CDF [10] showed that, for $BR_{b' \to bZ} = 1$, $m_{b'} > 199$ GeV/c^2.

In this note, b' pair production at LEP-II is considered within a sequential four generations model for $m_{b'} = 96 - 103$ GeV/c^2. Both the FCNC ($b' \to bZ$) and CC ($b' \to cW$) decay modes are studied. Different final states, corresponding to different b' decay modes

and subsequent decays of the Z and W bosons, are analysed, leading to limits on $BR_{b' \to bZ}$ and $BR_{b' \to cW}$. These limits, together with the theoretical predictions, are used to set exclusions on the plane $(R_{CKM}, m_{b'})$.

The different analyses are described in section 3. Results are presented in section 4.

2 Data samples and event generators

The analysed data were collected with the DELPHI detector [11] during the 1999 and 2000 LEP-II runs at $\sqrt{s} = 196 - 209$ GeV and correspond to an integrated luminosity of 420 pb^{-1}. The luminosity collected at each centre-of-mass energy is shown in Table 1. During the year 2000, DELPHI suffered from a problem in a sector (1/12 of the acceptance) of the Time Projection Chamber (TPC). This required modifications of the pattern recognition and affected the quality of charged track reconstruction [12]. Although the effect on the present analysis is small, these data were analysed separately in order to control any systematic difference.

$\sqrt{s}$ (GeV)	196	200	202	205	207	206*
luminosity (pb^{-1})	76.0	82.7	40.2	80.0	81.9	59.2

Table 1: *Luminosity collected with the DELPHI detector at each centre-of-mass energy. The data collected during the year 2000 with the TPC fully operational were split into two energy bins, below and above* $\sqrt{s} = 206$ GeV, *with* $\langle\sqrt{s}\rangle = 204.8$ GeV *and* $\langle\sqrt{s}\rangle = 206.6$ GeV, *respectively. The energy bin labeled 206* corresponds to the data collected with a sector of the TPC turned off and have* $\langle\sqrt{s}\rangle = 206.3$ GeV.

SM background processes were generated at each centre-of-mass energy using several simulation programs. All the four-fermion final states (both neutral and charged currents) were generated with WPHACT [13], while particular phase space regions of $e^+e^- \to e^+e^-f\bar{f}$, referred to as two-photon interactions, were generated using PYTHIA [16]. The $qq(\gamma)$ final state was generated with KK2F [14]. Bhabha events were generated with BHWIDE [15].

Signal samples were generated with PYTHIA 6.200 [17]. Although PYTHIA does not provide FCNC decay channels for quarks, it is possible to activate them by modifying the decay products of an available channel. The angular distributions assumed for b' pair production and decay were those predicted by the SM for any heavy down-type quark.

The generated signal and background events were passed through the detailed simulation of the DELPHI detector [11] and then processed with the same reconstruction and analysis programs as the real data. The Monte Carlo samples of the different background processes corresponded to several times the luminosity of the real data.

3 Analysis

The b' pair production has been searched for in both the FCNC ($b' \to bZ$) and CC ($b' \to cW$) decay modes. The b' decay modes and the subsequent decays of the gauge bosons (Z or W) generate several different final states (Fig. 2). The considered final states

and their branching ratios are summarized in Table 2. In all final states there are two jets originated by the two low energy b (FCNC) or c (CC) quarks.

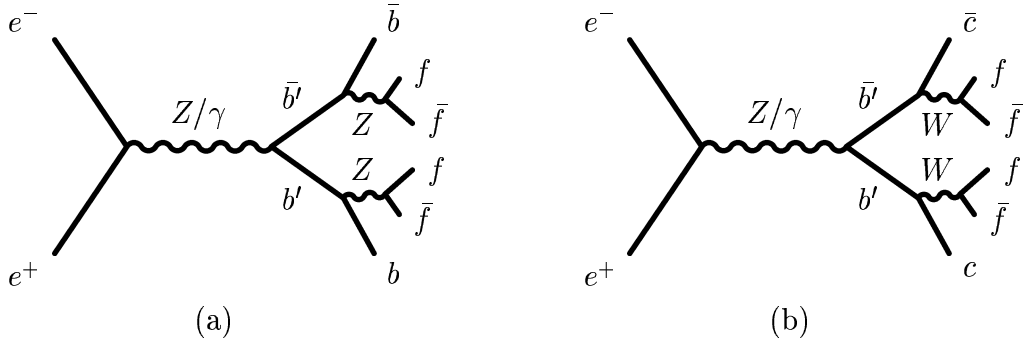

Figure 2: *Feynman diagrams corresponding to the b' (a) FCNC and (b) CC decay modes.*

b' decay	bosons decay	BR (%)	final states
$b' \to bZ$ (FCNC)	$ZZ \to ll\nu\bar{\nu}$	4.0	$bbll\nu\bar{\nu}$
	$ZZ \to q\bar{q}\nu\bar{\nu}$	28.0	$b\bar{b}q\bar{q}\nu\bar{\nu}$
	$ZZ \to q\bar{q}q\bar{q}$	48.6	$b\bar{b}q\bar{q}q\bar{q}$
$b' \to cW$ (CC)	$WW \to q\bar{q}l\bar{\nu}$	43.7	$c\bar{c}q\bar{q}l\bar{\nu}$
	$WW \to q\bar{q}q\bar{q}$	45.8	$c\bar{c}q\bar{q}q\bar{q}$

Table 2: *Considered final states corresponding to different b' decay modes (FCNC or CC) and subsequent decay of the gauge bosons (Z or W). About 81% (90%) of the branching ratio of the FCNC (CC) channels was covered.*

For all topologies events were required to have a visible momentum measured above 20° in polar angle[1] greater than $0.2\sqrt{s}$, and at least eight good charged tracks[2]. All the events were clustered into two, four or six jets by the Durham jet algorithm [18]. In order to reject monojet events, the resolution variable in the $2 \to 1$ jets transition, $y_{cut}(2 \to 1)$, was required to be above 0.2. Although two b jets are always present in the FCNC final states, they have a relatively low energy and the b-tagging was not used.

The electron, muon and photon identification was based on the standard DELPHI algorithms [11, 19]. Isolated leptons (photons) were defined by constructing double cones centered around the axis of the charged particle track (neutral cluster) with half opening angles of 5° and 25° (5° and 15°). To ensure isolation, the average energy density in the outer cone was required to be below 15 MeV/degree (10 MeV/degree). In the case of neutral deposits, no charged particle with more than 25 MeV was allowed inside the inner cone. The energy of the isolated particle was then re-evaluated as the sum of the energies

[1]In the standard DELPHI coordinate system, the z axis is along the electron direction. The polar angle is defined with respect to the z axis and it is represented as θ. Due to the detector symmetry, whenever a cut in polar angle is applied, the cut on the complementary angle is also done.

[2]Good charged tracks are selected by requiring a momentum above 0.1 GeV/c with a relative error below 1, and impact parameters along the beam direction and in the transverse plane below 4 cm and below 4 cm/$\sin\theta$ respectively.

inside the inner cone. For well identified leptons or photons the above requirements were weakened. In this case the angle of the external cone, α, was varied according to the energy of the lepton (photon) candidate, down to 2° for $p_{lepton} \geq 70$ GeV (3° for $E_\gamma \geq 90$ GeV), with the energy allowed inside the cone to be reduced proportionally to $\sin(\alpha)/\sin(25°)$ ($\sin(\alpha)/\sin(15°)$).

The number of isolated leptons and the missing energy were used to avoid overlaps between topologies. Whenever there were leptons in the final state (FCNC $b\bar{b}l\bar{l}\nu\bar{\nu}$ and CC $c\bar{c}q\bar{q}l\bar{\nu}$), events were divided into different samples, according to the lepton flavour identification:

1. *e sample*: well identified electrons;
2. *μ sample*: well identified muons;
3. *no-id sample*: leptons with non-identified flavour or two leptons identified with different flavours.

Specific cuts were used for each of the final states. A sequential cut analysis was adopted for the $b\bar{b}l\bar{l}\nu\bar{\nu}$ final state. For all other final states, a set of sequential cuts was followed by a discriminant analysis. In this case, a signal likelihood, $\mathcal{L}_S$, and a background likelihood, $\mathcal{L}_B$, were constructed for each in a set of relevant variables, neglecting correlations. The ratio $\mathcal{L}_S/\mathcal{L}_B$ was used as discriminant variable.

3.1 The $b\bar{b}l\bar{l}\nu\bar{\nu}$ final state

The FCNC $b\bar{b}l\bar{l}\nu\bar{\nu}$ final state is characterized by the presence of two low energy jets, two energetic leptons and a large missing energy. Both the invariant mass of the two leptons and the missing mass are expected to be around m_Z. All the events were clustered into two jets and only those with two leptons in the final state were accepted. The effective centre-of-mass energy [20], $\sqrt{s'}$, was required to be above $0.5\sqrt{s}$ and below $0.95\sqrt{s}$. Furthermore, in order to reject Bhabha background, the *no-id* sample events were required to have $|\cos\theta_{l1,l2}| < 0.86$, where $\theta_{l1,l2}$ are the polar angles of the first and second lepton[3], and no photons were allowed.

The number of data events and background expectation at this first selection level are given in Table 3. The distributions of some relevant variables are shown in Fig. 3.

The final selection was done by requiring the momenta of the first and second jets to be below 30 GeV/c and 12.5 GeV/c, respectively. Events in the e and *no-id* samples had to have a missing energy greater than $0.4\sqrt{s}$. μ sample events were required to have an angle between the two muons greater than 125°. Furthermore, in the *no-id* sample, the angle between the two leptons had to be greater than 140° and $p_{mis}/E_{mis} > 0.4$, where p_{mis} and E_{mis} are the missing momentum and energy.

At this level, one data event (0.8±1.1 expected from SM) was selected. This event belongs to the *no-id* sample and was collected at a centre-of-mass energy of about 200 GeV.

[3]The leptons and jets present in the events were numbered in order of decreasing energy.

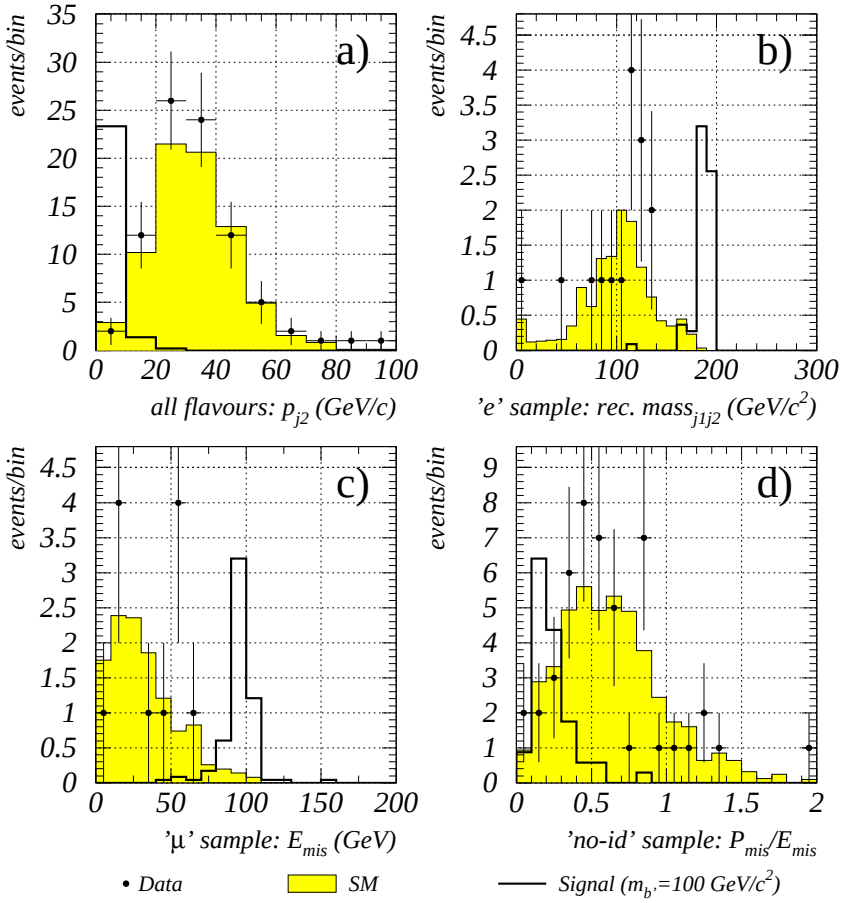

Figure 3: *$b\bar{b}l\bar{l}\nu\bar{\nu}$ final state: comparison of data (points) and SM simulation (shaded histogram) at $\sqrt{s} = 202 - 209$ GeV after the first selection level. (a) e+μ+"no-id" samples: momentum of the second jet; (b) e sample: recoil mass against the two jets; (c) μ sample: missing energy; (d) "no-id" sample: p_{mis}/E_{mis}, where p_{mis} and E_{mis} are the missing momentum and energy, respectively. Signal distributions ($m_{b'} = 100$ GeV/c^2, $\sqrt{s} = 205$ GeV) are also shown with arbitrary normalization.*

$\sqrt{s}$ (GeV)	data (SM expectation $\pm$ statistical error)		
	e	μ	*no-id*
196	2 (4.2±0.5)	1 (4.4±0.4)	21 (16.2±1.0)
200	5 (4.3±0.6)	4 (4.3±0.4)	15 (16.0±1.0)
202	4 (1.7±0.2)	1 (2.4±0.2)	7 (8.1±0.5)
205	4 (4.1±0.5)	4 (4.0±0.4)	16 (15.9±1.0)
207	4 (4.2±0.5)	5 (4.3±0.5)	21 (14.8±1.0)
206*	3 (2.9±0.3)	3 (2.7±0.3)	14 (10.8±0.7)
total	22 (21.4±1.1)	18 (22.1±0.9)	94 (81.8±2.1)

Table 3: *$b\bar{b}l\bar{l}\nu\bar{\nu}$ final state: number of events selected in data and SM expectation after the first selection level for each sample and centre-of-mass energy.*

3.2 The $b\bar{b}q\bar{q}\nu\bar{\nu}$ final state

This final state is characterized by the presence of four jets and a missing mass around m_Z. The events were clustered into four jets and were accepted if they had at least 20 good tracks, no leptons or photons and missing energy above 50 GeV. Furthermore, it was required that $-\log_{10}[y_{cut}(4 \to 3)] < 2.8$ and $\sqrt{s'} < 0.5\sqrt{s}$. The energy of the most energetic track of the first jet was required to be below $0.1\sqrt{s}$.

A fit imposing energy-momentum conservation was performed and the background like events with $\chi^2/n.d.f. < 6$ (Fig. 4a) were rejected. Table 4 summarizes the number of data candidates and expected SM background events at the preselection level.

Figs. 4b-d show, for this selection level, some relevant distributions of data and expected SM events at $\sqrt{s} = 202 - 205$ GeV.

$\sqrt{s}$ (GeV)	data (SM expectation $\pm$ statistical error)
196	123 (106.3±4.0)
200	111 (104.8±4.0)
202	50 (49.8±1.9)
205	88 (94.2±3.7)
207	99 (91.2±3.6)
206*	62 (65.7±2.6)
total	533 (511.7±8.3)

Table 4: *$b\bar{b}q\bar{q}\nu\bar{\nu}$ final state: number of events selected in data and SM expectation for each centre-of-mass energy at the preselection level.*

After the preselection, a likelihood ratio was defined, based on the probability density functions (PDFs) of the following variables:

- missing mass;
- $A_{cop}^{qq} \times \min(\sin\theta_{q1}, \sin\theta_{q2})$, where A_{cop}^{qq} is the acoplanarity, defined in the plane transverse to the beam, and $\theta_{q1,q2}$ are the polar angles of the jets when forcing the events

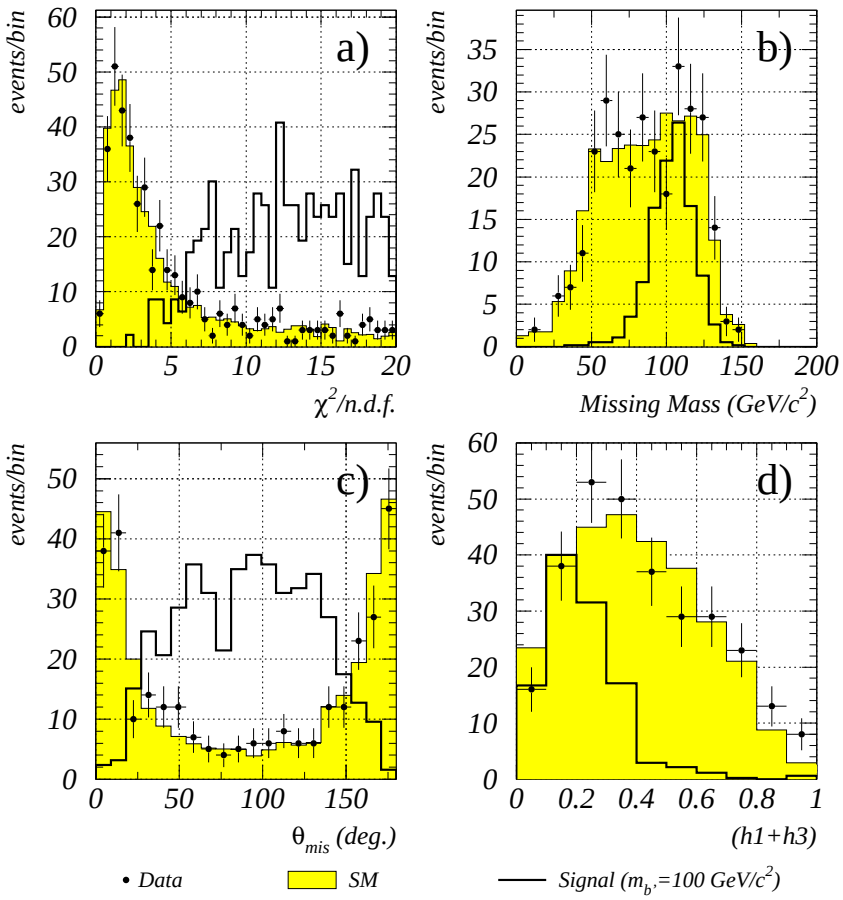

Figure 4: *$b\bar{b}q\bar{q}\nu\bar{\nu}$ final state: comparison of data (points) and SM simulation (shaded histogram) for $\sqrt{s} = 202 - 209$ GeV. (a) χ^2/n.d.f. of the fit imposing energy-momentum conservation (before the χ^2/n.d.f. cut); (b) missing mass; (c) polar angle of the missing momentum and $(h1 + h3)$ Fox-Wolfram momenta sum at the preselection level. Signal event distributions ($m_{b'} = 100$ GeV/c^2, $\sqrt{s} = 205$ GeV) are also shown with arbitrary normalization.*

into two jets[4];

- $180° - \alpha_{j1j2}$, where α_{j1j2} is the angle between the two most energetic jets;
- $h_1 + h_3$, where $h_{1,3}$ are the first and third Fox-Wolfram momenta [21];
- the polar angle of the missing momentum.

3.3 The $b\bar{b}q\bar{q}q\bar{q}$ final state

The FCNC $b\bar{b}q\bar{q}q\bar{q}$ final state is characterized by the presence of six jets and a small missing energy. All the events were clustered into six jets and only those with at least 30 good tracks, no isolated leptons and less than 50 GeV of missing energy were accepted. Moreover, events were required to have $\sqrt{s'} > 0.6\sqrt{s}$ and $-\log_{10}[y_{cut}(6 \to 5)] < 3.6$. The number of events selected in data and SM expectation are given in Table 5. Data, SM expectation and signal distributions of some relevant variables are shown in Fig. 5.

$\sqrt{s}$ (GeV)	data (SM expectation $\pm$ statistical error)
196	349 (326.7±5.3)
200	347 (342.1±5.5)
202	165 (162.1±2.6)
205	322 (319.0±5.2)
207	287 (307.6±5.0)
206*	192 (215.8±3.6)
total	1662 (1673.9±11.4)

Table 5: *$b\bar{b}q\bar{q}q\bar{q}$ final state: number of events selected in data and SM expectation for each centre-of-mass energy at the preselection level.*

The variables used to build the PDFs were:

- $-\log_{10}[y_{cut}(4 \to 3)]$;
- $-\log_{10}[y_{cut}(5 \to 4)]$;
- $h1 + h3$;
- $180° - \alpha_{j1j2}$, where α_{j1j2} is the angle between the two most energetic jets, with the event forced into four jets;
- momentum of the most energetic jet;
- angle between the two most energetic jets.

[4]While the four jets topology characterizes the signal, the two jets configuration is used in the background rejection.

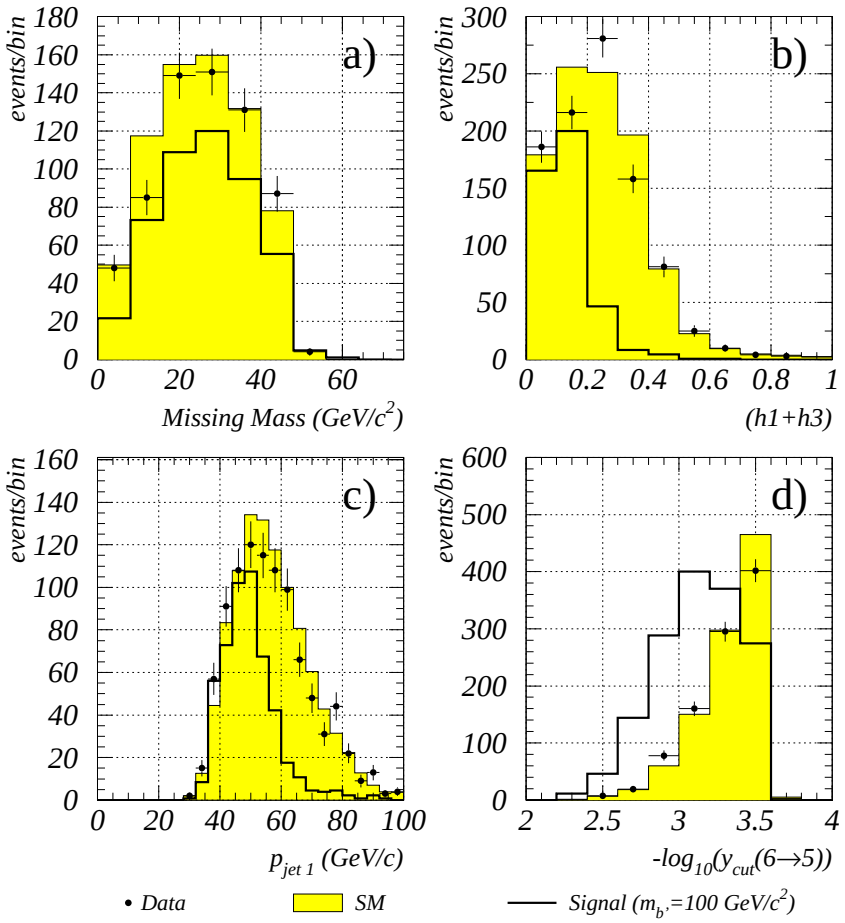

Figure 5: *$b\bar{b}q\bar{q}q\bar{q}$ final state: comparison of data (points) and SM simulation (shaded histogram) for $\sqrt{s} = 202 - 209$ GeV at the preselection level. (a) missing mass, (b) $(h1 + h3)$ Fox-Wolfram momenta sum, (c) momentum and (d) $-\log_{10}[y_{cut}(6 \to 5)]$ Durham resolution variable. Signal event distributions ($m_{b'} = 100$ GeV/c^2, $\sqrt{s} = 205$ GeV) are also shown with arbitrary normalization.*

3.4 The $c\bar{c}q\bar{q}l\bar{\nu}$ final state

The signature of the CC $c\bar{c}q\bar{q}l\bar{\nu}$ final state is the presence of four jets (two of them having low energy), one isolated lepton and missing energy. Events were clustered into four jets and were required to have at least 15 good tracks. No photons were allowed and one isolated lepton with momentum above 10 GeV/c and with a polar angle greater than 25° was required. Furthermore, they had to have only one track associated to the lepton and the most energetic track assigned to the first jet with momentum below $0.1\sqrt{s}$.

The number of data candidates and SM expectation for each sample (e, μ and *no-id*) are summarized in Table 6. The distributions of some relevant variables for data, background and signal are shown in Fig. 6.

$\sqrt{s}$ (GeV)	data (SM expectation ± statistical error)		
	e	μ	*no-id*
196	65 (51.1±1.4)	53 (56.1±1.5)	38 (34.4±1.4)
200	54 (58.1±1.7)	63 (59.9±1.6)	40 (35.0±0.7)
202	30 (27.8±0.8)	21 (28.4±0.8)	13 (16.9±0.7)
205	56 (50.8±1.5)	66 (53.6±1.5)	32 (33.3±1.4)
207	53 (53.8±1.6)	48 (57.2±1.6)	35 (33.8±1.4)
206*	31 (37.2±1.4)	42 (39.3±1.1)	21 (23.4±1.0)
total	289 (278.8±3.5)	293 (294.5±3.4)	179 (176.8 ± 2.8)

Table 6: *$c\bar{c}q\bar{q}l\bar{\nu}$ final state: number of events selected in data and SM expectation at the preselection level for each sample and centre-of-mass energy.*

The PDFs used to calculate the background and signal likelihoods were based on the following variables:

- $h1 + h3$;
- the invariant mass of the two jets, with the events forced into two jets;
- $-\log_{10}[y_{cut}(4 \to 3)]$;
- the sum of the momenta of all tracks in the hemisphere of the lepton;
- $180° - \alpha_{j1j2}$, where α_{j1j2} is the angle between the two most energetic jets;
- the angle between the lepton and the missing momentum.

In order to improve efficiency, events with no leptons seen in the detector were kept in a fourth sample. For this sample, the cuts of the $bb\nu\nu qq$ final state (section 3.2) were used and the same set of variables used to build the PDFs was adopted.

3.5 The $c\bar{c}q\bar{q}q\bar{q}$ final state

This final state is very similar to $b\bar{b}q\bar{q}q\bar{q}$ (with slightly different kinematics due to the mass difference between the Z and the W). Consequently the same analysis was adopted (see

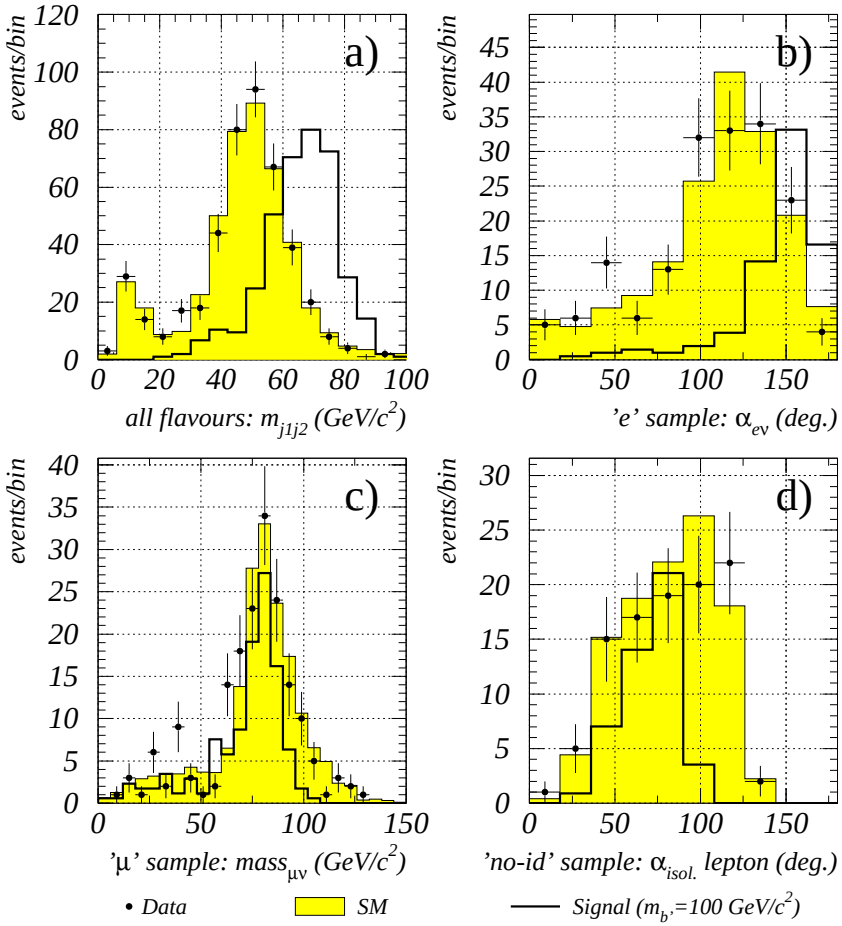

Figure 6: *$c\bar{c}q\bar{q}l\bar{\nu}$ final state: comparison of data (points) and SM simulation (shaded histogram) for $\sqrt{s} = 202 - 209$ GeV at the preselection level. (a) e+μ+"no-id" samples: invariant mass of the first and second jet; (b) e sample: angle between the electron and the missing momentum; (c) μ sample: invariant mass of the muon and missing momentum/energy; (d) "no-id" sample: isolation angle of the lepton. Signal event distributions ($m_{b'} = 100$ GeV/c^2, $\sqrt{s} = 205$ GeV) are also shown with arbitrary normalization.*

section 3.3). The number of selected events and SM expectation can be found in Table 5. The PDFs were built using the same set of variables.

4 Results

In the $b\bar{b}l\bar{l}\nu\bar{\nu}$ final state, one data event (0.8±1.1 expected from SM) was selected after the final selection level.

Discriminant analyses were used for all other final states. In these cases, signal, $\mathcal{L}_S$, and background likelihoods, $\mathcal{L}_B$, were constructed for the preselected events using the previously refered PDFs.

The distributions of of the discriminant variables, $\ln(\mathcal{L}_S/\mathcal{L}_B)$, for data and simulation (SM and signal) in the different final states are shown in Fig. 7.

The signal efficiencies, ε, and the branching ratio for the decay of the gauge bosons for each final state are shown in Table 7. The overall signal efficiency is the product of ε and the branching ratio for the decay of the gauge bosons.

final state	ε (%)
$bbll\nu\bar{\nu}$	
e sample	7.5±0.9
μ sample	10.1±1.0
no-id sample	5.0±0.7
$bbq\bar{q}\nu\bar{\nu}$	53.6±2.3
$bbq\bar{q}q\bar{q}$	63.4±2.5
$c\bar{c}q\bar{q}l\bar{\nu}$	
e sample	10 ± 1.0
μ sample	14.6 ± 1.2
no-id sample	4.2±0.6
no lepton sample	6.2±0.8
$c\bar{c}q\bar{q}q\bar{q}$	62.7±2.5

Table 7: *Signal efficiencies, ε, at the preselection level (final level for $b\bar{b}l\bar{l}\nu\bar{\nu}$) for each of the analysed final states. Overall signal efficiency is the product of ε and the branching ratio for the decay of the gauge bosons (Table 2). The error in ε is the statistical error. These efficiencies are constant within the error for all $\sqrt{s}$ and $m_{b'}$.*

Assuming the SM cross section for pair production of heavy quarks at LEP [17], limits at 95% confidence level on $BR_{b'\to bZ}$ (Fig. 8, upper plot) and $BR_{b'\to cW}$ (Fig. 8, lower plot) were obtained. These limits were evaluated using the modified frequentist likelihood method [22] based on the number of events remaining after applying cuts on $\ln(\mathcal{L}_S/\mathcal{L}_B)$. The cuts were chosen to keep high efficiency in all channels.

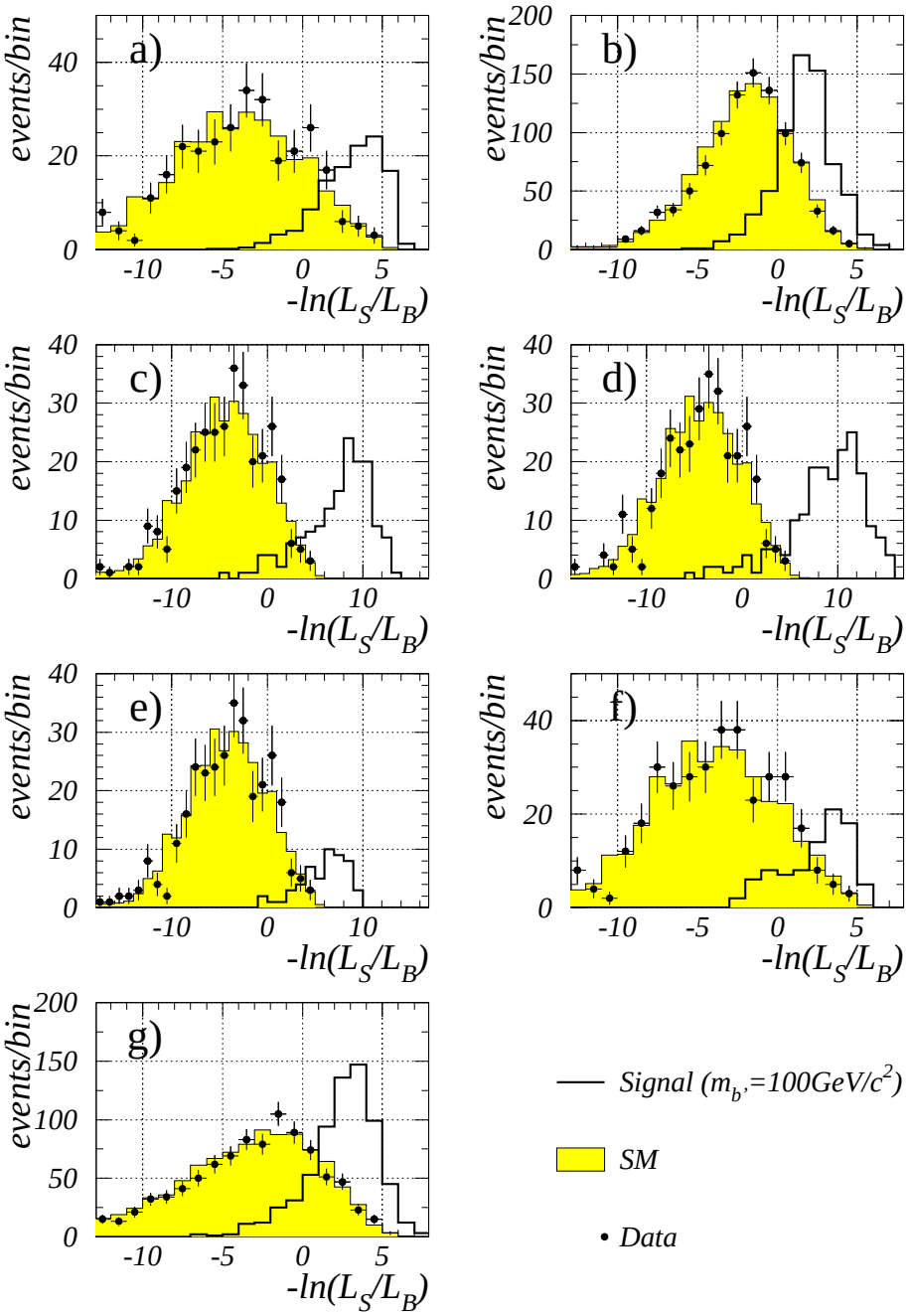

Figure 7: *Discriminant variables,* $\ln(\mathcal{L}_S/\mathcal{L}_B)$ *for the selected data events (points) and SM simulation (shaded histogram) for the different final states at* $\sqrt{s} = 202 - 209$ *GeV. FCNC* b' *decay mode: (a)* $b\bar{b}q\bar{q}\nu\bar{\nu}$ *and (b)* $b\bar{b}q\bar{q}q\bar{q}$*. CC* b' *decay mode: (c)* $c\bar{c}q\bar{q}l\bar{\nu}$ *(e sample), (d)* $c\bar{c}q\bar{q}l\bar{\nu}$ *(*μ *sample), (e)* $c\bar{c}q\bar{q}l\bar{\nu}$ *("no-id" sample) (f)* $c\bar{c}q\bar{q}l\bar{\nu}$ *("no lepton seen in detector") and (g)* $c\bar{c}q\bar{q}q\bar{q}$*.* $\ln(\mathcal{L}_S/\mathcal{L}_B)$ *is also shown for signal events generated with* $m_b = 100$ *GeV*$/c^2$ *and* $\sqrt{s} = 205$ *GeV. Signal normalization is arbitrary.*

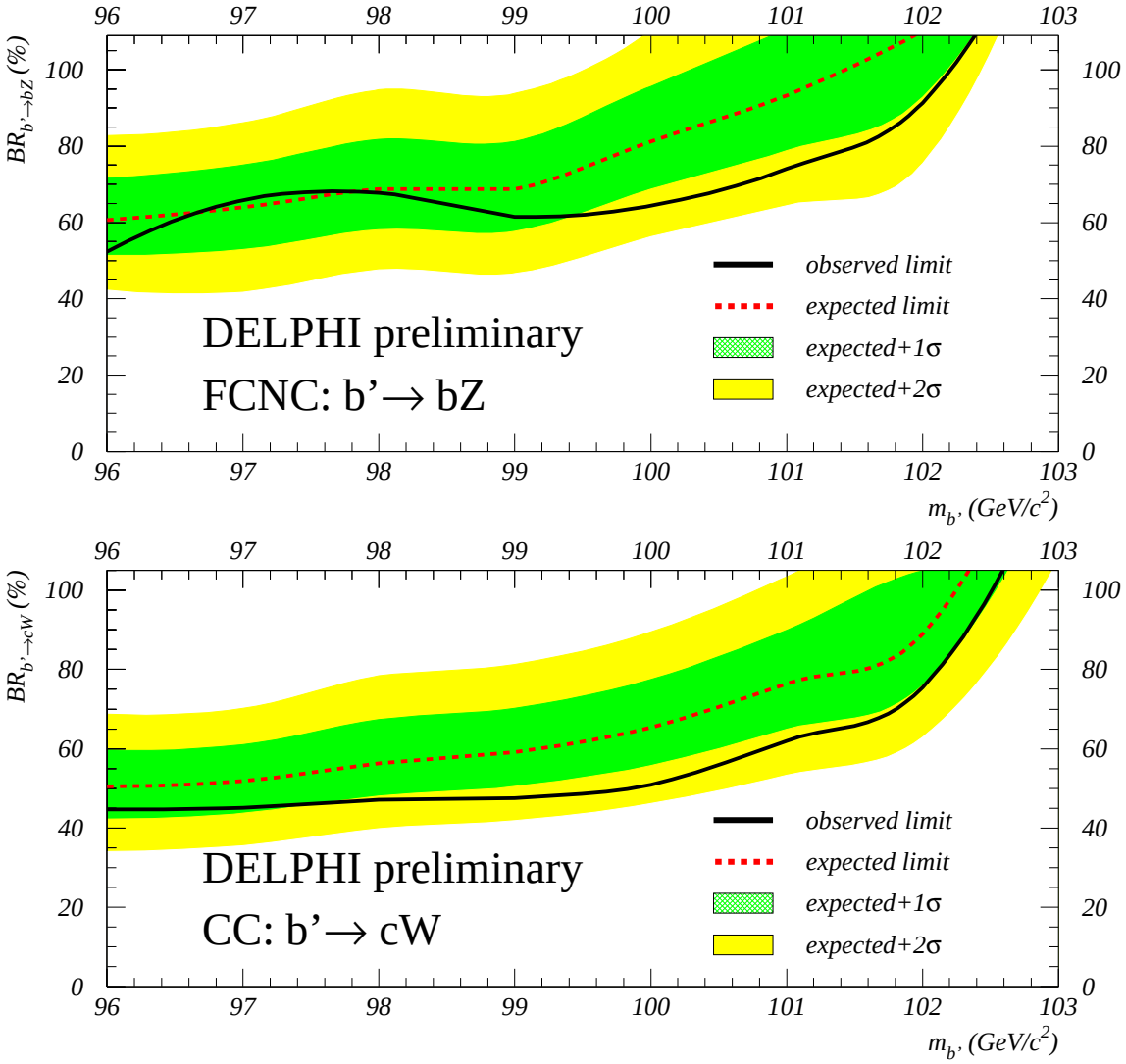

Figure 8: *Observed and expected (median) upper limits at 95% confidence level on* $BR_{b'\to bZ}$ *(upper plot) and* $BR_{b'\to cW}$ *(lower plot). The* 1σ *and* 2σ *bands around the expected median limit are also shown. These limits were computed as* $\sqrt{\frac{N_{signal}}{\mathcal{L}\times\sigma(e^+e^-\to b'\bar{b'})}}$*, where* N_{signal} *is the upper limit on the number of signal events,* $\mathcal{L}$ *is the data luminosity and* $\sigma(e^+e^- \to b'\bar{b'})$ *is the SM cross section for the pair production of heavy quarks at LEP.*

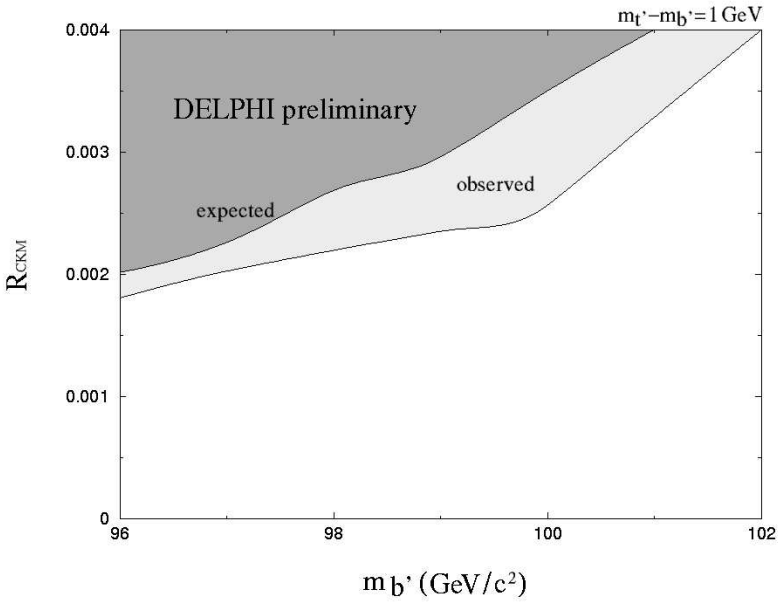

Figure 9: *95% confidence level excluded region in the plane (R_{CKM}, $m_{b'}$) with $m_{t'} - m_{b'} = 1$ GeV, obtained from the limits on $BR_{b' \to bZ}$ (bottom) and $BR_{b' \to cW}$ (top). The light and dark shadings correspond to the observed and expected median limits, respectively.*

5 Constraints on R_{CKM}

The theoretical branching ratios for the b' decays can be calculated within a four generations sequential model [5, 6, 7]. As stated before, if the b' is lighter than both the t and the t' quarks and $m_Z < m_{b'} < m_H$, the main contributions to the b' width are $\Gamma_{b' \to b\,Z}$ and $\Gamma_{b' \to c\,W}$. Nevertheless, the two-body decays $b' \to b\,\gamma$, $b' \to b\,g$ and the three body decays $b' \to b\,e^+\,e^-$, $b' \to b\,\nu\,\bar{\nu}$ and $b' \to b\,q\,\bar{q}$ can give a significant contribution to the total decay width.

Using the unitarity of the CKM matrix, its symmetry ($V_{t'b'}\,V_{t'b} \approx V_{tb}\,V_{tb'}$), its diagonality ($V_{ub'}\,V_{ub} \approx 0$) and taking $V_{cb} \approx 10^{-2}$ [23][5], the branching fractions of all possible b' decays can be written as a function of three variables: $R_{CKM} = |\frac{V_{cb'}}{V_{tb'}\,V_{tb}}|$ and the b' and t' masses [5, 6, 7].

Fixing $m_{t'} - m_{b'}$, bounds at 95% confidence level on R_{CKM} as a function of $m_{b'}$ can be drawn, using the limits on the branching ratios presented in section 4 (Fig. 8). Two extreme cases were considered: the almost degenerate case, where $m_{t'} - m_{b'} = 1$ GeV/c^2 (Fig. 9), and the case where the mass difference is close to the largest possible value, $m_{t'} - m_{b'} = 50$ GeV/c^2 [3, 5]. In Figs. 9 and 10, the upper curve in the ($R_{CKM}, m_{b'}$) plane is obtained from the limit on $\Gamma_{b' \to cW}$. The lower curve is related to $\Gamma_{b' \to bZ}$, which decreases with growing $m_{t'}$. This suppression is due to the GIM mechanism as $m_{t'}$ approaches m_t.

As $m_{b'}$ decreases, the lower limit on R_{CKM} becomes less stringent (Fig. 10) due to

[5]The two last conditions do not play a significant role in the final result. Using a very large value like, for instance, $V_{ub'}\,V_{ub} \approx 10^{-4}$ the contribution to the $b' \to b\,Z$ decay width is less than 1%.

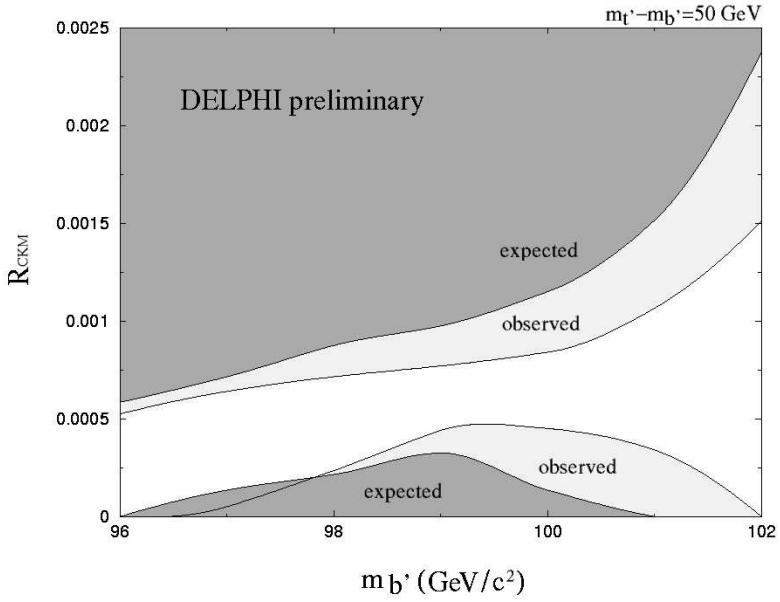

Figure 10: *95% confidence level excluded region in the plane (R_{CKM}, $m_{b'}$) with $m_{t'}-m_{b'} =$ 50 GeV, obtained from the limits on $BR_{b'\to bZ}$ (bottom) and $BR_{b'\to cW}$ (top). The light and dark shadings correspond to the observed and expected median limits, respectively.*

the competing neutral currents. Close to the $Z\,b$ threshold ($\approx$ 96 GeV/c^2), $b' \to b\,g$ dominates over $b' \to b\,Z$ and the theoretical $BR_{b'\to b\,Z}$ drops far below the experimental limit. However, as one moves away from the $Z\,b$ threshold, $b' \to b\,Z$ becomes the dominant neutral current.

6 Conclusions

The data collected with the DELPHI detector at $\sqrt{s} = 196 - 209$ GeV show no evidence for the pair production of b'-quarks with masses ranging from 96 to 103 GeV/c^2.

Assuming the SM cross section for pair production of heavy quarks at LEP, 95% confidence level upper limits on $BR_{b'\to bZ}$ and $BR_{b'\to cW}$ were obtained. These limits, combined with the theoretical predictions within a sequential fourth generation model, were used to exclude large parts of the(R_{CKM}, $m_{b'}$) plane for two hypotheses on the $m_{t'} - m_{b'}$ mass difference.

References

[1] LEP Electroweak Working Group, SLD Heavy Flavour Group, ALEPH, DELPHI, L3 and OPAL Coll., Abbaneo D. *et al.*, *Combination of Preliminary Electroweak Measurements and Constraints on the Standard Model*, LEPEWWG/2003-01 (2003).

[2] Novikov V.A., Okun L.B., Rozanov A.N. and Vysotsky M.I., *Phys. Lett.* **B529**, 111 (2002).

[3] Frampton P.H., Hung P.Q. and Sher M., *Phys. Rep.* **330**, 263(2000).

[4] Djouadi A. *et al.* in *Electroweak symmetry breaking and new physics at the TeV scale*, ed. Barklow, Timothy - World Scientific, Singapore (1997).

[5] Arhib A. and Hou W.S., *Phys. Rev* **D64**, 073016 (2001).

[6] Hou W.S. and Stuart R.G., *Phys. Rev. Lett.* **62**, 617 (1989);
Hou W.S. and Stuart R.G., *Nucl. Phys.* **B320**, 277 (1989);
Hou W.S. and Stuart R.G., *Nucl. Phys.* **B349**, 91 (1991).

[7] Oliveira S.M. and Santos R., *Bounds on the mass of b'-quark revisited*, in preparation.

[8] ALEPH Coll., Decamp D.*et al.*, *Phys. Lett.* **B236**, 511 (1990);
DELPHI Coll., Abreu P. *et al.*, *Nucl. Phys.* **B367**, 511 (1991);
L3 Coll., Adriani O. *et al.*, *Phys. Rep.* **236**, 1 (1993);
OPAL Coll., Akrawy M.Z. *et al.*, *Phys. Lett.* **B246**, 285 (1990).

[9] DØ Coll., Abachi S. *et al.*, *Phys. Rev.* **D52**, 4877 (1995).

[10] CDF Coll., Affolder T. *et al.*, *Phys. Rev. Lett.* **84**, 835 (2000).

[11] DELPHI Coll., Aarnio P. *et al.*, *Nucl. Instr. Meth.* **A303** (1991) 233;
DELPHI Coll., Abreu P. *et al.*, *Nucl. Instr. Meth.* **A378** (1996) 57.

[12] Elsing M. *et al.*, *Changes in the track reconstruction to recover from the TPC sector 6 failure*, DELPHI-2001-004 TRACK/95, 2001.

[13] Accomando E. and Ballestero A., *Comp. Phys. Comm.* **99** (1997) 270.

[14] Jadach S., Ward B.F.L. and Was Z., *Comp. Phys. Comm.* **130** (2000) 260.

[15] Jadach S., Płaczek W. and Ward B.F.L., *Phys. Lett.* **B390** (1997) 298.

[16] Sjöstrand T., *Comp. Phys. Comm.* **82** (1994) 74;
Sjöstrand T., *PYTHIA 5.7 and JETSET 7.4*, CERN-TH/7112-93.

[17] Sjöstrand T. *et al.*, *Comp. Phys. Comm.* **135** (2001) 238.

[18] Catani S. *et al.*, *Phys. Lett.* **B269** (1991) 432.

[19] Cossutti F. *et al.*, *REMCLU: a package for the Reconstruction of ElectroMagnetic CLUsters at LEP200*, DELPHI Note 2000-164 PROG 242.

[20] DELPHI Coll., Abreu P. et al., *Nucl. Instr. Meth.* **A427** (1999) 487.

[21] Fox G. and Wolfram S., *Phys. Lett.* **B82** (1979), 139.

[22] DELPHI Coll., Read A.L., DELPHI 97-158 PHYS 737 (1997);
Read A.L., CERN report 2000-005 (2000) 81.

[23] Hagiwara K. *et al.*, *Phys. Rev.* **D66** (2002), 010001.